SCIENTIFIC REPORTS

OPEN

SUBJECT AREAS:
BIOMEDICAL ENGINEERING
AXON AND DENDRITIC GUIDANCE
LAB-ON-A-CHIP
MAGNETIC TWEEZERS

Received
18 August 2014

Accepted
3 November 2014

Published
24 November 2014

Correspondence and requests for materials should be addressed to G.U.L. (gil.lee@ucd.ie)

Low Piconewton Towing of CNS Axons against Diffusing and Surface-Bound Repellents Requires the Inhibition of Motor Protein-Associated Pathways

Devrim Kilinc, Agata Blasiak, James J. O'Mahony & Gil U. Lee

UCD Nanomedicine Centre, School of Chemistry and Chemical Biology, University College Dublin, Belfield, Dublin 4, Ireland.

Growth cones, dynamic structures at axon tips, integrate chemical and physical stimuli and translate them into coordinated axon behaviour, *e.g.*, elongation or turning. External force application to growth cones directs and enhances axon elongation *in vitro*; however, direct mechanical stimulation is rarely combined with chemotactic stimulation. We describe a microfluidic device that exposes isolated cortical axons to gradients of diffusing and substrate-bound molecules, and permits the simultaneous application of piconewton (pN) forces to multiple individual growth cones *via* magnetic tweezers. Axons treated with Y-27632, a RhoA kinase inhibitor, were successfully towed against Semaphorin 3A gradients, which repel untreated axons, with less than 12 pN acting on a small number of neural cell adhesion molecules. Treatment with Y-27632 or monastrol, a kinesin-5 inhibitor, promoted axon towing on substrates coated with chondroitin sulfate proteoglycans, potent axon repellents. Thus, modulating key molecular pathways that regulate contractile stress generation in axons counteracts the effects of repellent molecules and promotes tension-induced growth. The demonstration of parallel towing of axons towards inhibitory environments with minute forces suggests that mechanochemical stimulation may be a promising therapeutic approach for the repair of the damaged central nervous system, where regenerating axons face repellent factors over-expressed in the glial scar.

Growth cones are highly dynamic tips of elongating axons that continuously probe their environment for both long and short range guidance cues, which may be either attractive or repulsive[1]. Guidance signals modulate the dynamics of actin filaments and microtubules in growth cones, which determines the subsequent axon behaviour, *i.e.*, elongation, turning, or retraction[2]. The role of mechanics in nervous system development, particularly in axon elongation, has recently been revisited (See recent reviews by Suter and Miller[3] and by Franze[4]). Growth cones drive themselves forward by generating tension and actively pulling on adhesions they form with their substrate[5]. Growth cone advance is a result of dynamic changes in the cytoskeleton and the activity of molecular motors, coordinated by a variety of signalling pathways. For example, external forces acting on cell adhesion molecules (CAMs) have been shown to affect actin dynamics through Src kinase signalling[6], which regulates integrin-mediated mechanotransduction, and through the RhoA-RhoA kinase (ROCK)-myosin II pathway, which regulates the actin arc structures that coordinate the microtubule organization in the growth cone[7]. Despite recent progress[4], how axonal growth cones translate mechanical stimuli into intracellular signalling is not fully understood.

Mechanical tension initiates and maintains neurite outgrowth *in vitro*[8], where the neurite elongation rate is a linear function of applied force above a minimum threshold[9]. Although directed axon initiation and outgrowth *via* external mechanical force application has been demonstrated[9,10], the effects of the physical and chemical environment on tension-induced axon outgrowth are not fully understood[11]. Magnetic tweezers (MTW) technique is based on the non-invasive manipulation of magnetic particles *via* externally-imposed magnetic fields[12]. MTW has been utilized to initiate and elongate neurites, where mechanical tension was applied *via* beads coated with integrin antibodies[10]. An electromagnet with a sharp tip and magnetic beads 4.5 μm in diameter were required to achieve 220–680 pN force that resulted in sustained axon elongation. However, the requirement of the electromagnet means that only one growth cone can be pulled at a time, which makes it highly inefficient to

combine force application with other experimental paradigms. This calls for an experimental model system that permits multiple growth cones to be pulled simultaneously.

Axon repellents are essential for the successful development and functioning of the nervous system. Semaphorin 3A (Sema3A) is a classical axon repellent which guides cortical axons during development, through binding its transmembrane receptor Neuropilin-1[13]. Sema3A causes growth cone collapse and axon retraction mediated by RhoA-ROCK pathway through the activation of myosin II and through the regulation of the actin cytoskeleton[14]. Local protein synthesis[15] and calpain activation[16] have also been shown to mediate Sema3A-induced growth cone collapse. Chondroitin sulfate proteoglycans (CSPGs), a class of extracellular matrix molecules, modulate growth cone morphology and inhibit axon growth through inhibiting the phosphorylation of phosphoinositide 3-kinase[17]. Substrate-bound CSPGs repel axons through inactivating integrin signalling[18] and through activating the RhoA-ROCK pathway[19]. Inhibition of RhoA, ROCK, or myosin II has been shown to promote central nervous system (CNS) axon elongation on CSPG-coated substrates[20,21]. Kinesin-5 is present in adult CNS axons and restricts axon growth by modulating the force balance on microtubules as well as their axonal transport[22]. Kinesin-5 inhibition has been shown to enhance axon elongation on both permissive and CSPG-coated substrates[22]. The involvement of multiple pathways in the axonal response to repellents calls for *in vitro* model systems that precisely control the growth cone microenvironment to understand the complex interactions between regulatory pathways, motor proteins, and the cytoskeleton.

There are common signalling pathways in axons downstream of repellent factors and external force application. Interfering with these pathways may direct and enhance the growth of axons that are simultaneously subjected to repellent cues and external forces. This possibility has direct implications for the repair of the injured CNS, where endogenous axon regeneration is prohibited by the inhibitory molecules that are over-expressed by the glial scar formation, such as Sema3A[23] and CSPGs[24]. In this context, an *in vitro* model system that enables the mechanical stimulation of multiple growth cones while exposing them to repellent factors may provide an excellent means to scan therapeutic candidates that promote axon extension into hostile environments. Axonal growth cones are typically exposed to gradients of chemotactic cues *in vivo* and have been shown to be highly sensitive to the steepness of guidance cue gradients[25]. This suggests that a successful *in vitro* model system should be able to incorporate gradients of both diffusing and substrate bound repellents.

There is a growing interest in microfluidic cell culture devices since they provide superior control over the physical and chemical microenvironment, compared to the classical *in vitro* cell culture. Microfluidic devices have been used to form concentration gradients either using a cascade of parallel laminar flows[26] or by flanking a cell culture channel between source and sink channels that are interconnected with a series of parallel microchannels that permit molecular diffusion[27]. Parallel microchannels can also be used to physically isolate axons from their cell bodies, by exploiting their sheer size difference, resulting in the subcellular compartmentalization of the neuron culture[28]. This principle has been applied to several neurobiology problems including synapse formation[29] and axon guidance[21,27]. By combining axon isolation with diffusion-based gradients, which form in the axon elongation direction, one can mimic the post-injury chemical environment, where regenerating axons face the inhibitory glial scar. In addition, the use of microfluidic compartmentalization provides an easy access to isolated growth cones for targeting multiple growth cones with magnetic particles.

We present a multiplexed *in vitro* model system which simultaneously applies near-horizontal tensile forces to a large number of axonal growth cones that can be treated independent of their cell bodies and be exposed to diffusing and surface-bound axon repellents. We show that, when combined with local inhibition of the ROCK pathway, low pN forces are sufficient to tow axons against Sema3A and CSPG gradients, thus suggesting that simultaneous mechanical and chemical stimulation of individual growth cones may lead to synergistic axon growth behaviour.

Results

Growth cone targeting and parallel magnetic tweezers force application. We have constructed a compartmentalized microfluidic device composed of three parallel chambers that are interconnected via parallel microchannels, which permit the passage of neurites but not of somata (Fig. 1a–1e). Mouse embryonic cortical neurons extend axons into the axonal chamber such that hundreds of individual growth cones can be found in the axonal chamber at 4-7 DIV. To apply uniform pulling forces, we synthesized superparamagnetic beads 1–2 μm in diameter that have high magnetization and are uniform in size (CV $<$ 5%), using a novel microfluidics method (Supplementary Fig. S1; see Supplementary Information for details). The microfluidic neuron culture device permitted us to use a particle-NdBFe dipole magnet distance of 2.5–3 mm, which corresponds to 11–12 pN horizontal pulling force per 1.4 μm bead (Supplementary Fig. S2)[30].

When the bead suspension is introduced into the axonal chamber, beads functionalized with an antibody against neural CAM (NCAM) preferentially targeted growth cones where NCAM is localized (Figs. 1f and 1g). After 10–15 min of incubation, most beads were observed to be attached to the central domains of the growth cones, suggesting that they first bind to the peripheral domains and are concentrated through coupling with the retrograde actin flow. Beads were also observed be immobilized to axon shafts and in some cases travelled swiftly along the axon when pulled with a lateral force of 8–9 pN (Supplementary Fig. S3a; Supplementary Movie S1), suggesting that the particles bind to membrane receptors that are not necessarily linked to the underlying cytoskeleton. Beads that were non-specifically attached to the PLL-coated substrate were occasionally picked up by the filopodia of the growth cones of elongating axons (Supplementary Fig. S3b; Supplementary Movie S2). Horizontal forces less than 12 pN in magnitude did not have a drastic effect on axon elongation. However, in agreement with earlier studies[9–11], forces in excess of 80 pN were able to accelerate axon elongation considerably (Supplementary Fig. S3c; Supplementary Movie S3). Two different elongation behaviours were observed when growth cones were pulled with 6–12 pN force. In 80% of cases, the bead did not engage with the growth cone and remained in its original position while the axon elongated (Supplementary Fig. S3d; Supplementary Movie S4). In 20% of cases, the bead engaged with the growth cone and towed the growth cone at an increased rate in the force direction (Fig. 1h, Supplementary Movie S5). In this case, towed axons continued to grow after the force application had stopped (Supplementary Fig. S4). These results show that microfluidic isolation permits the targeting and parallel pulling of a high number of growth cones with uniform horizontal forces.

Axons exhibit different elongation responses to uniform and gradient Sema3A. A linear concentration gradient forms in the axonal chamber when the molecule of interest is provided to the distal chamber (Fig. 2a). The gradient (dC/dx) and the mid-chamber concentration (C_{50}) stabilized in 30 min after the addition of equal volumes of media to the wells and remained stable for at least 3 h (Supplementary Fig. S5). Assuming that 70 kDa dextran and Sema3A have similar diffusion coefficients, we calculate the stabilized dC/dx and C_{50} to be 0.24 nM/mm and 0.20 nM, respectively, for 57 nM distal Sema3A treatment. Growth cones were subjected either to uniform Sema3A, delivered directly to the axonal chamber, or to the Sema3A gradient. Unlike other model systems[2,14], Sema3A did not cause growth cone collapse or axon

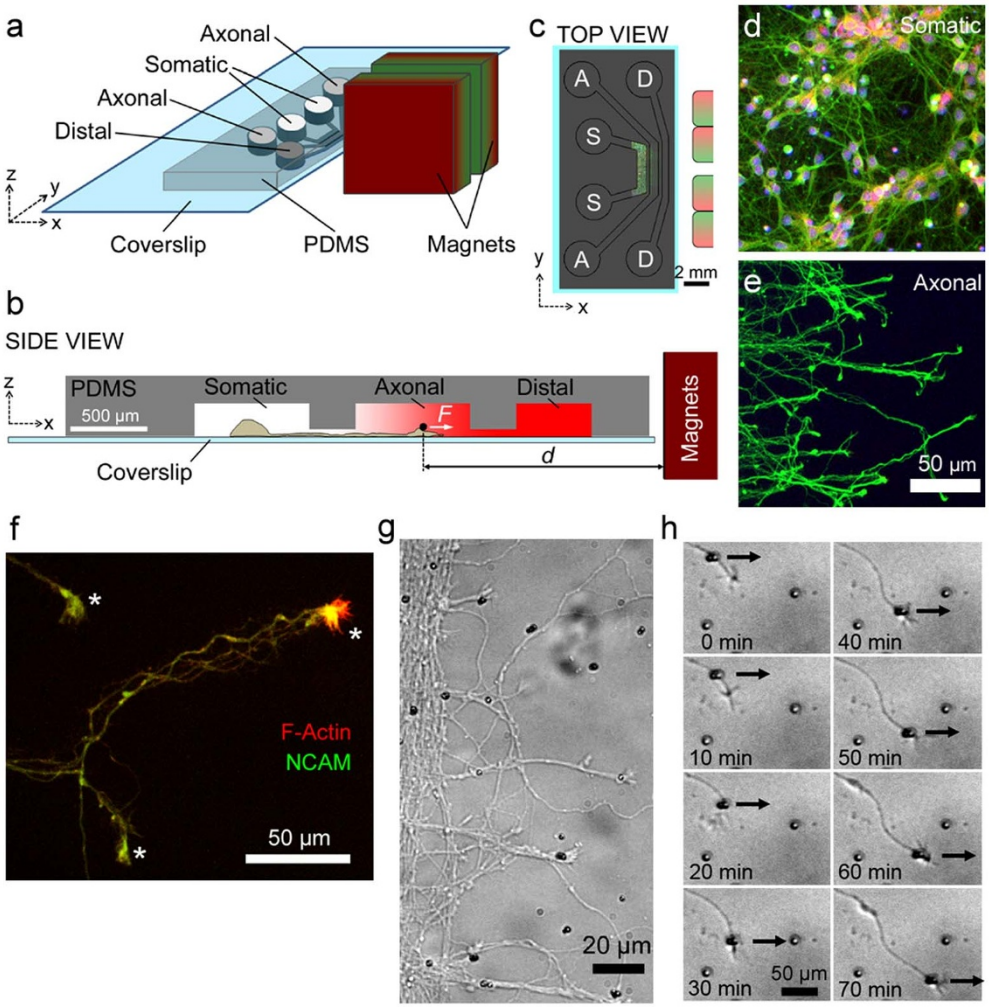

Figure 1 | Experimental model for parallel axon towing against chemical gradients, integrated to an optical microscope. (*a*). The schematic of the three-compartmental (somatic, axonal, distal) neuron culture device and the dipolar NdBFe magnet assembly. (*b*). The side view of the device showing the distance from the edge of the magnet assembly to the middle of the axonal chamber, *d*, which is used to estimate the force (*F*) acting on magnetic particles. Chamber and channel heights are not in scale. (*c*). The top view of the microfluidic device superposed with a micrograph of immunostained mouse cortical neurons fixed after 6 days in culture, showing β3-tubulin (green), actin filaments (red), and nuclei (blue). S, A, and D indicate the somatic, axonal, and distal chambers, respectively. (*d–e*). Micrographs of immunostained mouse cortical neurons at 6 days in vitro (DIV), showing β3-tubulin (green), actin filaments (red), and nuclei (blue), acquired from the somatic and axonal chambers. (*f*). NCAM localization to growth cones shown at 5 DIV. Stars indicate growth cone locations with strong NCAM immunolabeling. (*g*). Targeting of axonal growth cones with particles functionalized with NCAM antibody. (*h*). An example of axon towing where 9.2 pN force was directed parallel to microchannels (arrow direction).

retraction in developing cortical neurons (Supplementary Fig. S6). However, Sema3A did cause a slight decrease in axon speed (Supplementary Fig. S7) and a more pronounced decrease in the x-component of the velocity vector, V_x (Figs. 2f and 2g). This suggests that Sema3A does not block the motility of the cortical axons but decreases the net distance they parse in their forward advance direction, parallel to the microchannels. The change in the axon elongation direction was analyzed by comparing the early (30–60 min) and the late (90–120 min) periods of Sema3A treatment. Here, a positive angle indicates a deviation away from the Sema3A source, regardless of the sign of the deviation angle the axon makes. Sema3A gradient, but not the uniform Sema3A treatment caused a significant deviation (Figs. 2f and 2h). The deviation, but not the retardation of axons in response to Sema3A gradient, was dose-dependent.

Axons slow down on CSPG coated substrates. The effect of CSPG on cortical axon elongation was studied by coating the axonal chamber with CSPG at increasing bulk concentrations, as quantified through immunostaining (Fig. 2b–2e). Axons entering the CSPG-coated axonal chamber exhibited a dose-dependent fasciculation and retardation similar to earlier reports[31]. Axons exhibited a slight decrease in their motility (Supplementary Fig. S7) and a pronounced decrease in their net forward progress, *i.e.*, V_x (Figs. 2f and 2g), consistent with the extent of invasion of the axonal chamber at 6DIV on different CSPG coatings. A CSPG gradient in the axonal chamber was generated by adding intermediate and high concentrations of CSPG to axonal and distal chambers, respectively (Supplementary Fig. S8). On CSPG gradients, axons not only slowed down, but also deviated away from the *x*-direction, *i.e.*, away from the higher CSPG density (Figs. 2f and 2h), similar to the Sema3A response.

Local treatment of axons with inhibitory drugs blocks axon repulsion induced by Sema3A or by CSPG. Growth cones exposed to diffusing Sema3A gradients were treated with a panel of inhibitory drugs delivered to the axonal chamber only (Fig. 3 and Supplementary Figs. S9 and S10). Local protein synthesis[15] and

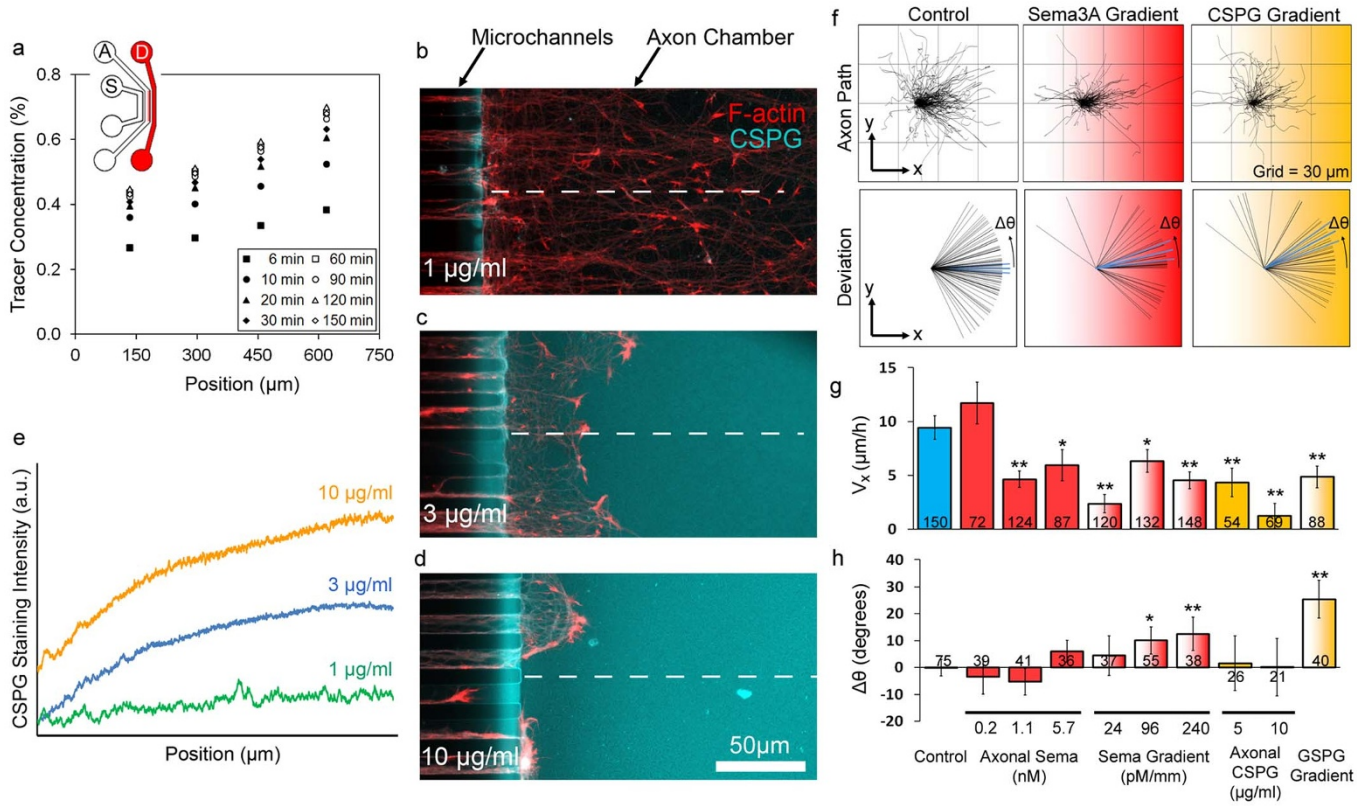

Figure 2 | Response of developing mouse cortical axons to Semaphorin 3A (Sema3A) and chondroitin sulfate proteoglycan (CSPG). (*a*). The concentration profile of 70 kDa fluorescent tracer molecule was expressed as a fraction of the distal concentration at indicated time points. Inset showing the gradient induction paradigm. S, A, and D indicate the somatic, axonal, and distal chambers, respectively. (*b–d*). Axon growth on CSPG-coated axonal chamber at 6 days in vitro (DIV) for varying CSPG stock concentrations. (*e*). The graph shows the CSPG immunostaining intensity along dashed lines shown in panels *b-d*. (*f*). Axon elongation maps were generated for controls, Sema3A gradient (0.24 nM/mm), and CSPG gradient (5 μg/ml axonal, 10 μg/ml distal) by recording the positions of individual growth cones every 10 min and superposing their starting points at the origin. The angular change in the axon elongation direction between early (30–60 min) and late (90–120 min) periods ($\Delta\theta$) plotted as unit vectors for each axon. Note that a negative $\Delta\theta$ means turning towards $+x$ axis and a positive $\Delta\theta$ means turning away from the $+x$ axis. The mean value of $\Delta\theta \pm$ standard error given as longer vectors (blue). (*g*). The *x*-component of the velocity vector (V_x) was calculated by dividing the net distance covered by the growth cone in the x-direction to the experiment duration. Solid and gradual coloring in bars represent bulk and gradient treatments, respectively for controls (blue), Sema3A (red) and CSPG (yellow). (*h*). Average angular deviation in the axon elongation direction for the same treatments. One-way ANOVA, followed by t-test, * $p < 0.05$, ** $p < 0.01$ compared to controls. Numbers on bars represent the number of individual axons analyzed.

calpain activation[16] have been proposed as mediators of Sema3A-mediated growth cone collapse and retraction. Similarly, RhoA-ROCK-myosin II pathway has been shown to be downstream of the Sema3A signalling pathway[14]. As shown in Fig. 3A, the decrease in V_x induced by Sema3A gradient was blocked when axons were treated with inhibitors of calpain, RhoA, ROCK, or myosin II. Among these, the myosin II inhibitor Blebbistatin (Bleb) had the most significant effect in V_x against the Sema3A gradient, which quadrupled and exceeded the average V_x of the untreated controls. However, Bleb was also observed to cause fast yet erratic axon elongation (Supplementary Figs. S9 and S10), excessive branching, and rapid growth cone turnover in control axons, similar to axons of myosin II knock-out mice[32]. The deviation in the elongation direction induced by Sema3A gradient was blocked with local treatments with calpain inhibitor ALLN or ROCK inhibitor Y-27632. ALLN and Y-27632 were therefore identified as candidate molecules to test for their capacity to promote force-induced axon elongation against Sema3A gradients.

Axons growing on CSPG gradients were also locally treated with a panel of inhibitory drugs. Treatment with Bleb blocked the CSPG-induced decrease in V_x. On the other hand, treatment with Y-27632 blocked the CSPG-induced deviation in the axon elongation direction. Despite its effects on the Sema3A response ALLN failed to block the retardation and deviation induced by CSPG. Kinesin-5 inhibition has been shown to enhance axon elongation on CSPG-coated substrates[22]. Accordingly, axonal treatment of monastrol, a specific inhibitor of kinesin-5, caused a slight improvement in V_x (no statistical significance), and reverted the CSPG-induced deviation in the axon elongation direction (Fig. 3). Y-27632 and monastrol were therefore identified as candidate molecules to test for their capacity to promote force-induced axon elongation on CSPG gradients.

Axon towing against Sema3A and CSPG gradients requires the inhibition of downstream pathways. In a subset of experiments, we applied tensile forces, 8–12 pN in magnitude, to axons that are subjected to Sema3A or CSPG gradients, and co-treated them with a panel of inhibitory molecules (Fig. 4 and Supplementary Fig. S11). In the control group, *i.e.*, without Sema3A or CSPG, axons that were engaged with magnetic beads upon force application exhibited 2.7× faster elongation (V_x), compared to axons that are not targeted or not engaged (Fig. 4a). When these axons were co-treated with Y-27632, force application increased the elongation rate by 3.6-fold (Fig. 4b). In axons that were subjected to Sema3A gradients, force application without co-treatment resulted in a slight increase (1.3×) in the elongation rate (Fig. 4c). In axons subjected to Sema3A gradients and co-treated with Y-27632, force application increased the

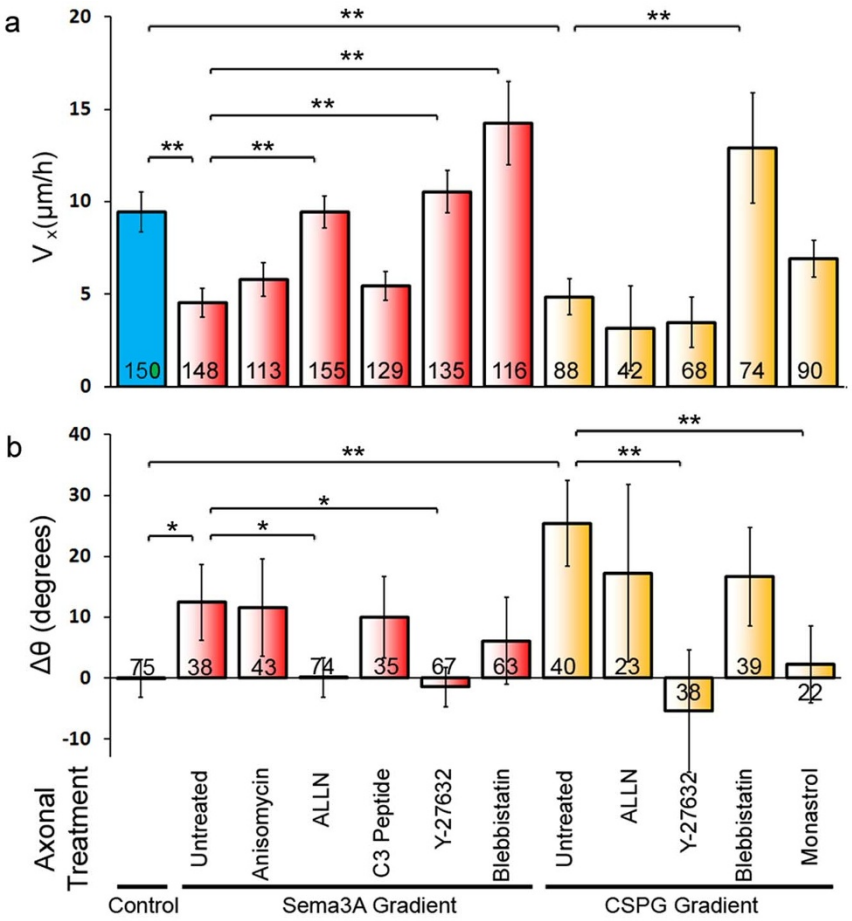

Figure 3 | Axonal response to Sema3A and CSPG gradients in combination with local axonal treatment with a panel of inhibitory molecules: Protein synthesis inhibitor Anisomycin (25 μM); calpain inhibitor ALLN (5 μM); RhoA inhibitor C3 peptide (0.5 μg/ml); ROCK inhibitor Y-27632 (10 μM); myosin II inhibitor Blebbistatin (50 μM); kinesin-5 inhibitor monastrol (100 μM). (*a*). The velocity vector in the *x*-direction, *i.e.*, against Sema3A (0.24 nM/mm; red) or CSPG (5 μg/ml axonal, 10 μg/ml distal; yellow) gradients, and in controls (green). (*b*). The angular deviation in the axon elongation direction between early (30–60 min) and late (90–120 min) periods for the same treatments. One-way ANOVA, followed by t-test, * $p < 0.05$, ** $p < 0.01$. Error bars represent standard error of the mean. Numbers on bars represent the number of individual axons analyzed.

elongation rate by 5.8-fold (Fig. 4d). Although ALLN alone blocked Sema3A-induced retardation and deviation in axons that were not pulled (Fig. 3), the elongation rates of pulled axons against Sema3A gradients did not change with ALLN co-treatment (Fig. 4i). In axons growing on CSPG gradients, growth cone pulling did not result in axon towing unless axons were co-treated with Y-27632 or monastrol (Figs. 4c–4e). Axons co-treated with Y-27632 or monastrol had 7.6× or 8.8× higher V_x, respectively (Figs. 4h–4i). Axonal Bleb treatment blocked the engagement of magnetic beads with growth cones, and was hence found to be counter-productive for force-induced axon growth. Cumulatively, these results indicate that external forces lower than 12 pN can successfully tow axons towards a source of axon repellents, if the downstream effectors of these repellent molecules are blocked.

Discussion

There is a growing interest in *in vitro* model systems that control the neuron microenvironment by independently controlling the stiffness, topography, or protein composition of the substrate. For example, synergistic effects on axon elongation have been observed when microtopographical cues were combined with surface bound growth factors[33] or with diffusible guidance cues[34]. However, model systems combining direct mechanical stimulation with chemical or topographical properties of the neuron microenvironment are lacking. Existing techniques for applying external forces to axonal growth cones allow studying only one axon at a time and are therefore not suitable for conducting complex experiments in which multiple parameters are studied[9,10]. To overcome this bottleneck, we established an *in vitro* model system that permits the application of tensile forces to a large number of CNS growth cones which are exposed to surface-bound or diffusing axon repellents and locally treated with a panel of inhibitory drugs. Using this model system we first identified a set of pathway inhibitors that interfere with the axonal response to select chemorepellents, and then tested for their capacity to promote axon towing against molecular gradients of these repellents.

Massively parallel magnetic tweezers force application has been successfully employed for biophysical assays at nucleic acid, protein, and cellular levels[12]. To our knowledge, this is the first study that employs parallel magnetic tweezers to pull on cells in the plane of their substratum. Each microfluidic circuit enabled *ca.* 25 individual axonal growth cones to be targeted with single beads, thereby permitting the mechanical pulling experiments to be run in parallel. The development of magnetic beads with considerably higher magnetization, compared to commercial beads, enabled significant forces to be achieved with magnetic field gradients that can be produced using commercial permanent magnets[35,36]. Particles 1.4 μm in diameter were chosen for this study to achieve pulling forces up to 22 pN, while minimizing the torque applied during near-horizontal force application. In summary, the model system presented here is capable of delivering uniform pulling forces over a large area within the

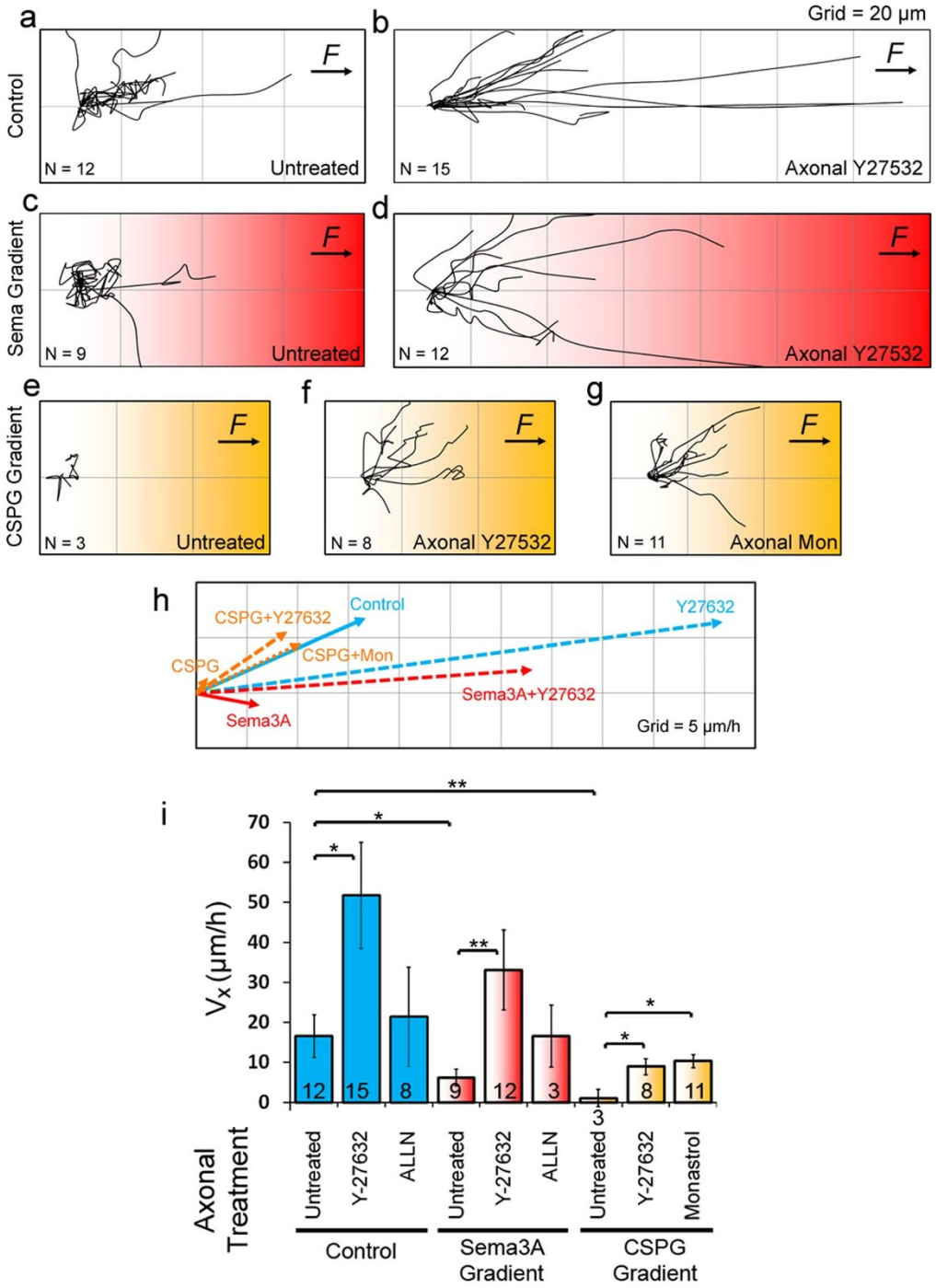

Figure 4 | Axon pulling with less than 12 pN force against gradients of inhibitory molecules. (*a–g*). Axon elongation maps were generated for growth cones that engage with magnetic particles by recording the positions of individual growth cones every 10 min and moving their starting points to the origin. Sema3A (0.24 nM/mm; red) and CSPG (5 μg/ml axonal, 10 μg/ml distal; yellow) gradients are formed in the *x*-direction. The concentrations of Y-27632 and monastrol were 10 μM and 100 μM, respectively. N is the number of towed axons. (*h*). Average velocity vector for axons shown in elongation maps. (*i*). The *x*-component of the velocity vector was calculated by dividing the net distance covered by the growth cone in the x-direction to the experiment duration. ALLN concentration was 5 μM. One-way ANOVA, followed by t-test, * $p < 0.05$, ** $p < 0.01$. Error bars represent standard error of the mean. Numbers on bars represent the number of individual axons analyzed.

microfluidic device (*ca.* 1 mm^2), such that high numbers of growth cones can be studied in parallel.

Early studies using glass needles to pull on growth cones showed that, beyond a minimum threshold, axon elongation rate was proportional to the applied tension, *i.e.*, 1 μm/h for every 10 pN[9]. Compared to chick dorsal root ganglion (DRG) neurons[8] or PC12 cells[37], chick forebrain neurons (CFNs) have been shown to have a lower tension threshold (50 pN) before their axons could be extended, *i.e.*, any tension above 50 pN led to axon towing[9]. Later studies where CFNs were pulled *via* magnetic beads coated with integrin antibodies suggested a lower force threshold (15 pN) and demonstrated that optimal neurite initiation and axon elongation occurred at 450 pN[10]. Our results show that intact mouse cortical neurons can be towed with less than 12 pN acting on the transmembrane NCAM, suggesting that

the dynamics of the force-induced growth depends on the neuron type and the receptor targeted. The rate of elongation increased 8.3 μm/h for every 10 pN, which is nearly one order of magnitude higher than has been reported previously[9].

During axon elongation the actin cytoskeleton of the growth cone generates contractile forces to pull on the focal adhesions it forms with the substratum. The average internal stress in the growth cone has been estimated to be 5.8 Pa (with dynamic stress peaks of 40.1 Pa) for NG108-15 neuroblastoma-glioma hybrid cells cultured on soft substrates (E = 0.2 kPa) by measuring the dynamic actin flow[38]. These growth cones generated an average peak traction stress of 26.7 Pa, measured *via* traction force microscopy, resulting in a net neurite pulling force of 0.6 nN[38]. Based on the Hertz theory[39], we estimate the minimum contact area between the particle and the growth cone due to the indentation caused by the weight of the bead to be 0.017 μm^2 (see Supplementary Information). However, the effective contact area may be higher due to the topographical heterogeneity in the growth cone and the partial engulfment of the bead through bond formation. If the pulling force is assumed to be equally distributed to the contact area, the stress generated by the typical magnetic tweezers pulling force in our experiments (12 pN) will be 0.7 kPa. This value is two orders of magnitude higher than the internal stress generated by growth cones[38,40]. Tensile stress has been suggested to activate the local intracellular environment in the vicinity of pulled receptors such that it becomes more receptive to growing microtubule tips[10]. The exploration of the growth cone periphery by microtubule +tips has been characterized as a random walk with minute timescales[41]; thus, pulling transmembrane receptors over long periods of time may result in the prolonged activation of the local environment. This would then increase the probability of microtubule docking and lead to force-mediated growth cone towing[10]. Indeed, tensile stress induced by forces acting on apCAM has been shown to result in the translocation and polymerization of microtubules towards the site of force application[7]. Therefore, not the total force *per se*, but the force per transmembrane molecule may be affecting axon growth. This would explain the striking difference between our data and previous reports in terms of elongation rate increase per applied force.

We show that forces that are two orders of magnitude lower than axonal resting tension can direct and accelerate axons if the axonal force generation machinery is compromised through the inhibition of molecular motors and related signalling, *i.e.*, ROCK pathway. *In vivo*, ROCK inhibition promotes axon regeneration and improves locomotor function following spinal cord transection[42]. *In vitro*, ROCK inhibition accelerates growth cone advance towards apCAM-coated beads, which were physically restrained to counteract the force exerted by the growth cone[7]. However, ROCK inhibition also reduces the directional coherence of actin filaments and is therefore considered to be a "double edged therapeutic sword," promoting growth at the expense of directional control[7]. Since the direction of the externally-applied force dominates the elongation direction in towed axons in this study, only one edge of this "therapeutic sword" would be used. In agreement with earlier studies using Ntera-2 cells[43], our results show that ROCK inhibition did not have any adverse effects on axon morphology (Fig. S10) or on axon elongation behaviour (Fig. S9). Interestingly, ROCK inhibition promoted neurite outgrowth in myelin-inhibited retinal ganglion cells only when co-treated with ciliary neurotrophic factor[44], but protected corticostriatal synapses following axotomy without requiring any co-treatment[45]. Further studies are required to determine the detailed molecular mechanisms of ROCK inhibition in axons.

Chemotaxis of axonal growth cones were suggested to depend on the steepness of the guidance cue gradient. For example, nerve growth factor (NGF) gradients as shallow as 0.1% have been shown to direct axons sprouting from rat DRG explants[25]. To establish molecular gradients, we relied on the passive diffusion of solutes and used the distal and somatic chambers of a tri-compartmental neuron device[46] as source and sink, respectively[47]. Although the source and sink concentrations were not kept constant during our experiments, the relatively large reservoir volumes provided an experimental window of at least 3 hours. 5.7 nM distal Sema3A treatment results in a Sema3A gradient of 24 pM/mm, which corresponds to 0.12% concentration difference across a 10 μm-diameter growth cone. While reducing axon velocity significantly, this treatment did not deflect axons. When the concentration difference was increased 10×, axons not only slowed down but were also deflected, confirming that axon guidance depends on the steepness of the molecular gradient. However, the steepness threshold may be different for the neuron type and guidance cue at hand[25]. Interestingly, in our hands axonal retardation and deflection response against CSPG gradients and against Sema3A gradients were similar, in agreement with the notion that common mechanisms involving the regulation of intracellular messengers mediate the axonal response to different repellents[48].

Mechanisms of axon repulsion in response to Sema3A and CSPG are being intensively studied[16,24]. Local protein synthesis has been shown to mediate growth cone response to Sema3A in retinal[15] and hippocampal[49] neurons. Calpains, Ca^{2+} dependent neutral proteases, have recently been shown to mediate Sema3A-induced growth cone collapse through cleaving and activating ion channels[16] and through truncating phosphorylated p53[50]. Finally, RhoA-ROCK-myosin II pathway has been shown to mediate Sema3A-induced growth cone response[2,14]. We therefore treated axons exposed to Sema3A with specific inhibitors of these pathways and assessed their effects on axon elongation. Based on experiments without force application, we identified ROCK inhibitor Y-27632 and calpain inhibitor ALLN as candidates for promoting axon towing against Sema3A gradients. Likewise, axons exposed to CSPGs were locally treated with a panel of inhibitory molecules. Among these, Myosin II inhibitor Bleb blocked CSPG-induced axon retardation, as suggested by others[21]. However, axon retardation was not blocked by ROCK inhibition, which promotes axon regeneration after optic nerve crush injury *in vivo*[43], or by kinesin-5 inhibition, which promotes axon elongation on CSPG *in vitro*[22]. In contrast, CSPG-induced axon deviation was blocked by inhibiting ROCK or kinesin-5, but not myosin II. Considering the lack of engagement of Bleb-treated growth cones with magnetic beads, Y-27632 and kinesin-5 inhibitor monastrol were identified as candidates for promoting axon towing against CSPG gradients. These results demonstrate the efficiency of the microfluidic device in testing a number of compounds for their effects on fluidically-isolated axons that are exposed to chemotactic or haptotactic cues.

We have discussed the hypothesis that tensile stress may be promoting directed axon elongation through generating a receptive environment for microtubule +tips in the vicinity of pulled receptors. It is conceivable that the growth cone cytoskeleton in developing axons is in a state of dynamic imbalance in terms of stress, which leads to spontaneous axon elongation. External factors such as repellent cue signalling and force application may be modulating the growth cone elongation behaviour through affecting this stress balance (Fig. 5). Our data provides several lines of evidence that support this idea. First, when the RhoA-ROCK pathway, which regulates the actomyosin contractility, was inhibited, force application increased the axon velocity 3.6× in control conditions, 5.8× against Sema3A, and 7.6× against CSPG. Second, when kinesin-5 was inhibited, force application increased the axon velocity 8.8× against CSPG. Kinesin-5 is a microtubule +tip directed motor protein, whose inhibition increases axon elongation rates through increasing the frequency of anterograde transport of short microtubules and enhancing the microtubule entry to distal regions[22]. Moreover, focal inhibition of kinesin-5 in the transition zone (between central and peripheral domains) promotes the invasion of the peripheral zone by

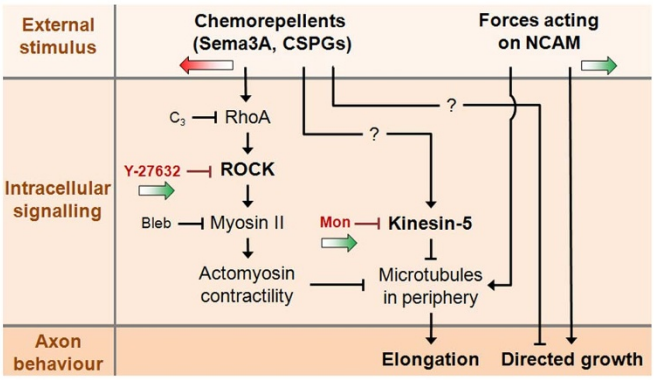

Figure 5 | Putative mechanisms of interaction between repellent cue signalling and focal mechanical stimulation towards regulating growth cone behaviour. The effects of external stimuli on the growth cone stress balance are indicated by green (tensile) and red (contractile) block arrows. According to this scenario, microtubule advance to growth cone periphery is promoted by inhibiting ROCK which reduces actomyosin contractility and by inhibiting myosin-5 which lowers anterograde forces acting on microtubules. On the other hand, external force acting on NCAM activates the local cellular environment such that the probability of microtubule docking is increased. The combination of inhibitors that promote microtubule advance and mechanical forces that promote microtubule docking promote directed axon growth despite repulsive signalling.

microtubules[51]. Therefore, (i) shifting the growth cone stress balance such that the retrograde forces on microtubules are lowered and (ii) simultaneously pulling on a small number of transmembrane CAMs such that a receptive environment for the microtubules is created in the vicinity of the bead may promote and direct axon growth towards repellent factors.

Localized trauma to CNS axons, *e.g.*, spinal cord injury (SCI), causes the degeneration of distal axons and results in glial scarring at the site of the lesion. Adult CNS axons have the potential to regenerate if provided with a suitable environment[52]; however, endogenous regeneration is prohibited by the glial scar which acts as a mechanical barrier as well as a source of axon repellents[53]. A successful repair strategy would involve a combination of approaches that minimize the inhibitory effects of the environment and maximize the intrinsic regenerative capacity of axons. Research is currently focused on therapies that combine engineered biomaterial scaffolds with cell transplantation and local delivery of neurotrophic factors[54]. Force-induced growth of regenerating axons through regions of low permissivity may be an alternative/supplementary therapeutic approach. In support of this idea, continuous stretch of integrated DRG neurons, *i.e.*, without growth cones, has been demonstrated by using a microstepper motor, where axons were grown as long as 10 cm[55]. These "extreme stretch grown" neurons were successfully implanted in rats to bridge severed sciatic nerves and shown to promote regeneration of the endogenous axons within months[56]. However, this technique is limited to integrated axons and may not be feasible for the repair of endogenous CNS, due to operational constraints imposed by the stretching device.

To be considered as a minimally invasive therapeutic approach, growth cone pulling needs to be demonstrated with particles small enough to freely navigate through the extracellular matrix. Using small particles and a uniform magnetic field to pull a high number of particles simultaneously would inherently decrease the applied force magnitude, but not so much the tensile stress. In magnetic tweezers force application, force and stress vary with the cube and the cube root of the particle diameter, respectively (see Supplementary Information), suggesting that despite the tiny forces generated, submicron beads may produce sufficient tensile stress to promote growth. Here we show that constant forces less than 12 pN acting on 1.4 μm-diameter beads attached to axon growth cones promote and direct elongation against gradients of Sema3A or CSPG, if axons are simultaneously treated with inhibitors of motor proteins or associated signalling pathways. Considering that both the diffusible Sema3A[23] and matrix-bound CSPG[24] are over-expressed in the glial scar, our results suggest that mechanochemical stimulation may be a novel therapeutic approach for promoting axon regrowth following CNS injury. Forces in this range may be generated *in vivo* by exposing magnetic particles to fields generated externally with or without using a magnetizable implant[57].

In conclusion, we show that multiple CNS growth cones can be targeted and simultaneously pulled by using NCAM-functionalized magnetic particles in a compartmentalized neuron culture device which also enables isolated treatment of axons. This allows for the testing of pharmaceutical compounds in combination with mechanical force application towards discovering synergistic interactions between mechanical and chemical treatments. Hence, the integration of MTW with microfluidics provides an excellent test bed for the rapid screening of biomolecules for their capacity to promote axon towing. Force application at magnitudes significantly lower than previously suggested, accelerate and direct axons when combined with the local inhibition of motor proteins or ROCK pathway. Modulating those pathways that regulate the contractile stress in axons and applying tensile stress through external forces acting on a small number of transmembrane receptors may by promoting microtubule advance into peripheral regions of the growth cone and driving axons forward. The combination of mechanical stimulation and pharmaceutical intervention promoted axon elongation against gradients of repellent molecules. Parallel towing of regenerating axons may thus be a promising strategy for developing minimally-invasive therapies to repair the injured CNS.

Methods

Details of all materials and experimental procedures, including cell culture and reagents, fabrication of microfluidic devices, and characterization of concentration gradients are described in Supplementary Information.

Magnetic particle synthesis and functionalization. Magnetic particles that consist of densely packed Fe_xO_y nanoparticles embedded in a polymer matrix and therefore possess a strong and highly uniform magnetization were synthesized *via* a novel, microfluidics-based method. Briefly, oil droplets were formed at the orifice of commercial microfluidic X-junction chip (Supplementary Fig. S1a; Dolomite, Royston, UK) and were let dry to form microparticles. Particles were coated with a polymer layer containing carboxyl groups using the layer-by-layer deposition technique[35]. The concentration of Fe_xO_y nanoparticles was used to control the particle diameter, which had a coefficient of variation less than 5% (Supplementary Fig. S1d). Magnetic particles were further coated with a layer of polyethylene glycol (PEG) to minimize non-specific interactions and conjugated with an antibody (Millipore) recognizing the extracellular portion of the mouse NCAM, using previously described protocols[58].

Microfluidic neuron culture and quantification of axon elongation. A three-compartmental microfluidic circuit (Fig. 1) similar to a previous design[46] was fabricated using photolithography. The procedures for obtaining primary cells were approved by the UCD Animal Research Ethics Committee. Cortical neurons isolated from E14 mouse embryos[46] were seeded in the somatic chamber, which extend axons through the microchannels. Axon elongation was quantified by tracking growth cones. The velocity vector was determined by dividing the distance between growth cone positions in the first and last timeframes to the duration of the experiment. The scalar velocity is the average instantaneous speed of the growth cone, calculated by dividing the distance covered between each consecutive time point to the time period between two timeframes (10 min). Finally, the turning angle was defined as the angle between the velocity vectors in the 30–60 min and 90–120 min time periods for axons with scalar velocities higher than 15 μm/h (25 μm/h for experiments with Bleb).

Magnetic tweezers force application to axonal growth cones. A permanent magnet assembly consisting of two pairs of NdFeB magnets with their same poles facing each other over a 1 mm air gap was used[58]. Force acting on particles was determined from their drag velocity in a viscous fluid as a function of distance from the magnet assembly (Supplementary Fig. S2b). A 1.4 μm-diameter magnetic bead located at 1.5 mm distance from the magnet assembly can apply 22 pN force. This is the shortest distance possible for a bead in the axonal chamber of the microfluidic device and therefore the highest force achievable in the current study. For growth cone

targeting, all reservoirs of the microfluidic devices were emptied. 4 μl Neurobasal medium was added to the top reservoirs of the somatic and distal chambers, followed by the addition of 4 μl particle suspension (0.1 g/L) to the top reservoir of the axonal chamber. Excess particles were rinsed with 10 μl medium after 10 min of incubation. Each reservoir was filled with 30 μl of experimental media and topped with 10 μl of dimethylpolysiloxane (100 cSt; Sigma) to minimize evaporation.

1. Tessier-Lavigne, M. & Goodman, C. S. The molecular biology of axon guidance. *Science* **274**, 1123–1133 (1996).
2. Kalil, K. & Dent, E. W. Touch and go: guidance cues signal to the growth cone cytoskeleton. *Curr Opin Neurobiol* **15**, 521–526 (2005).
3. Suter, D. M. & Miller, K. E. The emerging role of forces in axonal elongation. *Prog Neurobiol* **94**, 91–101 (2011).
4. Franze, K. The mechanical control of nervous system development. *Development* **140**, 3069–3077 (2013).
5. Lamoureux, P., Buxbaum, R. E. & Heidemann, S. R. Direct evidence that growth cones pull. *Nature* **340**, 159–162 (1989).
6. Suter, D. M. & Forscher, P. Transmission of growth cone traction force through apCAM-cytoskeletal linkages is regulated by Src family tyrosine kinase activity. *J Cell Biol* **155**, 427–438 (2001).
7. Schaefer, A. W. *et al.* Coordination of actin filament and microtubule dynamics during neurite outgrowth. *Dev Cell* **15**, 146–162 (2008).
8. Bray, D. Axonal growth in response to experimentally applied mechanical tension. *Dev Biol* **102**, 379–389 (1984).
9. Chada, S., Lamoureux, P., Buxbaum, R. E. & Heidemann, S. R. Cytomechanics of neurite outgrowth from chick brain neurons. *J Cell Sci* **110**, 1179–1186 (1997).
10. Fass, J. N. & Odde, D. J. Tensile force-dependent neurite elicitation via anti-beta1 integrin antibody-coated magnetic beads. *Biophys J* **85**, 623–636 (2003).
11. Lamoureux, P., Zheng, J., Buxbaum, R. E. & Heidemann, S. R. A cytomechanical investigation of neurite growth on different culture surfaces. *J Cell Biol* **118**, 655–661 (1992).
12. Kilinc, D. & Lee, G. U. Advances in magnetic tweezers for single molecule and cell biophysics. *Integr Biol (Camb)* **6**, 27–34 (2014).
13. Polleux, F., Giger, R. J., Ginty, D. D., Kolodkin, A. L. & Ghosh, A. Patterning of Cortical Efferent Projections by Semaphorin-Neuropilin Interactions. *Science* **282**, 1904–1906 (1998).
14. Gallo, G. RhoA-kinase coordinates F-actin organization and myosin II activity during semaphorin-3A-induced axon retraction. *J Cell Sci* **119**, 3413–3423 (2006).
15. Campbell, D. S. & Holt, C. E. Chemotropic responses of retinal growth cones mediated by rapid local protein synthesis and degradation. *Neuron* **32**, 1013–1026 (2001).
16. Kaczmarek, J. S., Riccio, A. & Clapham, D. E. Calpain cleaves and activates the TRPC5 channel to participate in semaphorin 3A-induced neuronal growth cone collapse. *Proc Natl Acad Sci U S A* **109**, 7888–7892 (2012).
17. Silver, L., Michael, J. V., Goldfinger, L. E. & Gallo, G. Activation of PI3K and R-Ras signaling promotes the extension of sensory axons on inhibitory Chondroitin sulfate proteoglycans. *Dev Neurobiol* **74**, 918–933 (2014).
18. Tan, C. L. *et al.* Integrin activation promotes axon growth on inhibitory chondroitin sulfate proteoglycans by enhancing integrin signaling. *J Neurosci* **31**, 6289–6295 (2011).
19. Borisoff, J. F. *et al.* Suppression of Rho-kinase activity promotes axonal growth on inhibitory CNS substrates. *Mol Cell Neurosci* **22**, 405–416 (2003).
20. Dergham, P. *et al.* Rho signaling pathway targeted to promote spinal cord repair. *J Neurosci* **22**, 6570–6577 (2002).
21. Hur, E. M. *et al.* Engineering neuronal growth cones to promote axon regeneration over inhibitory molecules. *Proc Natl Acad Sci U S A* **108**, 5057–5062 (2011).
22. Lin, S. *et al.* Inhibition of Kinesin-5, a microtubule-based motor protein, as a strategy for enhancing regeneration of adult axons. *Traffic* **12**, 269–286 (2011).
23. Pasterkamp, R. J. *et al.* Expression of the gene encoding the chemorepellent semaphorin III is induced in the fibroblast component of neural scar tissue formed following injuries of adult but not neonatal CNS. *Mol Cell Neurosci* **13**, 143–166 (1999).
24. Bartus, K., James, N. D., Bosch, K. D. & Bradbury, E. J. Chondroitin sulphate proteoglycans: key modulators of spinal cord and brain plasticity. *Exp Neurol* **235**, 5–17 (2012).
25. Rosoff, W. J. *et al.* A new chemotaxis assay shows the extreme sensitivity of axons to molecular gradients. *Nat Neurosci* **7**, 678–682 (2004).
26. Li Jeon, N. *et al.* Neutrophil chemotaxis in linear and complex gradients of interleukin-8 formed in a microfabricated device. *Nat Biotechnol* **20**, 826–830 (2002).
27. Bhattacharjee, N., Li, N., Keenan, T. M. & Folch, A. A neuron-benign microfluidic gradient generator for studying the response of mammalian neurons towards axon guidance factors. *Integr Biol (Camb)* **2**, 669–679 (2010).
28. Taylor, A. M. *et al.* A microfluidic culture platform for CNS axonal injury, regeneration and transport. *Nat Methods* **2**, 599–605 (2005).
29. Taylor, A. M., Dieterich, D. C., Ito, H. T., Kim, S. A. & Schuman, E. M. Microfluidic local perfusion chambers for the visualization and manipulation of synapses. *Neuron* **66**, 57–68 (2010).
30. Shang, H. & Lee, G. U. Magnetic tweezers measurement of the bond lifetime-force behavior of the IgG-protein A specific molecular interaction. *J Am Chem Soc* **129**, 6640–6646 (2007).
31. Snow, D. M., Smith, J. D., Cunningham, A. T., McFarlin, J. & Goshorn, E. C. Neurite elongation on chondroitin sulfate proteoglycans is characterized by axonal fasciculation. *Exp Neurol* **182**, 310–321 (2003).
32. Bridgman, P. C., Dave, S., Asnes, C. F., Tullio, A. N. & Adelstein, R. S. Myosin IIB is required for growth cone motility. *J Neurosci* **21**, 6159–6169 (2001).
33. Gomez, N., Lu, Y., Chen, S. & Schmidt, C. E. Immobilized nerve growth factor and microtopography have distinct effects on polarization versus axon elongation in hippocampal cells in culture. *Biomaterials* **28**, 271–284 (2007).
34. Kundu, A. *et al.* Superimposed topographic and chemical cues synergistically guide neurite outgrowth. *Lab Chip* **13**, 3070–3081 (2013).
35. O'Mahony, J. J., Platt, M., Kilinc, D. & Lee, G. Synthesis of superparamagnetic particles with tunable morphologies: the role of nanoparticle-nanoparticle interactions. *Langmuir* **29**, 2546–2553 (2013).
36. Li, P., Kilinc, D., Ran, Y. F. & Lee, G. U. Flow enhanced non-linear magnetophoretic separation of beads based on magnetic susceptibility. *Lab Chip* **13**, 4400–4408 (2013).
37. Lamoureux, P., Altun-Gultekin, Z. F., Lin, C., Wagner, J. A. & Heidemann, S. R. Rac is required for growth cone function but not neurite assembly. *J Cell Sci* **110**, 635–641 (1997).
38. Betz, T., Koch, D., Lu, Y. B., Franze, K. & Kas, J. A. Growth cones as soft and weak force generators. *Proc Natl Acad Sci U S A* **108**, 13420–13425 (2011).
39. Costa, K. D. Single-cell elastography: probing for disease with the atomic force microscope. *Dis Markers* **19**, 139–154 (2003).
40. Koch, D., Rosoff William, J., Jiang, J., Geller Herbert, M. & Urbach Jeffrey, S. Strength in the Periphery: Growth Cone Biomechanics and Substrate Rigidity Response in Peripheral and Central Nervous System Neurons. *Biophys J* **102**, 452–460 (2012).
41. Odde, D. J., Tanaka, E. M., Hawkins, S. S. & Buettner, H. M. Stochastic dynamics of the nerve growth cone and its microtubules during neurite outgrowth. *Biotechnol Bioeng* **50**, 452–461 (1996).
42. Fournier, A. E., Takizawa, B. T. & Strittmatter, S. M. Rho kinase inhibition enhances axonal regeneration in the injured CNS. *J Neurosci* **23**, 1416–1423 (2003).
43. Lingor, P. *et al.* Inhibition of Rho kinase (ROCK) increases neurite outgrowth on chondroitin sulphate proteoglycan in vitro and axonal regeneration in the adult optic nerve in vivo. *J Neurochem* **103**, 181–189 (2007).
44. Ahmed, Z., Berry, M. & Logan, A. ROCK inhibition promotes adult retinal ganglion cell neurite outgrowth only in the presence of growth promoting factors. *Mol Cell Neurosci* **42**, 128–133 (2009).
45. Deleglise, B. *et al.* Synapto-Protective Drugs Evaluation in Reconstructed Neuronal Network. *PLoS ONE* **8**, e71103 (2013).
46. Kilinc, D. *et al.* Wallerian-like degeneration of central neurons after synchronized and geometrically registered mass axotomy in a three-compartmental microfluidic chip. *Neurotox Res* **19**, 149–161 (2011).
47. Shamloo, A., Ma, N., Poo, M. M., Sohn, L. L. & Heilshorn, S. C. Endothelial cell polarization and chemotaxis in a microfluidic device. *Lab Chip* **8**, 1292–1299 (2008).
48. Horner, P. J. & Gage, F. H. Regenerating the damaged central nervous system. *Nature* **407**, 963–970 (2000).
49. Li, C., Bassell, G. J. & Sasaki, Y. Fragile X Mental Retardation Protein is Involved in Protein Synthesis-Dependent Collapse of Growth Cones Induced by Semaphorin-3A. *Front Neural Circuits* **3**, 11 (2009).
50. Qin, Q., Liao, G., Baudry, M. & Bi, X. Role of calpain-mediated p53 truncation in semaphorin 3A-induced axonal growth regulation. *Proc Natl Acad Sci U S A* **107**, 13883–13887 (2010).
51. Nadar, V. C., Lin, S. & Baas, P. W. Microtubule redistribution in growth cones elicited by focal inactivation of kinesin-5. *J Neurosci* **32**, 5783–5794 (2012).
52. David, S. & Aguayo, A. J. Axonal elongation into peripheral nervous system "bridges" after central nervous system injury in adult rats. *Science* **214**, 931–933 (1981).
53. Shoichet, M. S., Tate, C. C., Baumann, M. D. & LaPlaca, M. C. Strategies for regeneration and repair in the injured central nervous system environment. *Indwelling Neural Implants: Strategies for Contending with the In Vivo Environment* Reichert, W. M. (ed.) (CRC Press, Boca Raton, FL, 2008).
54. McCreedy, D. A. & Sakiyama-Elbert, S. E. Combination therapies in the CNS: engineering the environment. *Neurosci Lett* **519**, 115–121 (2012).
55. Pfister, B. J., Iwata, A., Meaney, D. F. & Smith, D. H. Extreme stretch growth of integrated axons. *J Neurosci* **24**, 7978–7983 (2004).
56. Huang, J. H. *et al.* Long-term survival and integration of transplanted engineered nervous tissue constructs promotes peripheral nerve regeneration. *Tissue Eng Part A* **15**, 1677–1685 (2009).
57. Polyak, B. *et al.* High field gradient targeting of magnetic nanoparticle-loaded endothelial cells to the surfaces of steel stents. *Proc Natl Acad Sci U S A* **105**, 698–703 (2008).

58. Kilinc, D., Blasiak, A., O'Mahony, J. J., Suter, D. M. & Lee, G. U. Magnetic tweezers-based force clamp reveals mechanically distinct apCAM domain interactions. *Biophys J* **103**, 1120–1129 (2012).

Acknowledgments

We thank Joe O'Brian for technical help. This study was supported by Science Foundation Ireland (08/RP1/B1376 and 08/IN1/B2072; G.U.L.), by the Irish Higher Education Authority (PRTLI Nanoremedies; G.U.L.), by the Tyndall National Institute (NAP-287; D.K. and G.U.L.), by a Marie Curie Intra-European Fellowship (D.K.), and by an AXA Research Fund Doctoral Fellowship (A.B.).

Author contributions

D.K. and G.U.L. designed research; D.K. performed the majority of experiments, J.J.M. synthesized and characterized magnetic particles; A.B. performed immunocytochemistry and characterized gradients; D.K. analyzed the data and wrote the paper; and G.U.L. wrote the paper and supervised the research. D.K. and G.U.L. share senior authorship of this work.

Additional information

Supplementary information accompanies this paper at http://www.nature.com/scientificreports

Competing financial interests: The authors declare no competing financial interests.

How to cite this article: Kilinc, D., Blasiak, A., O'Mahony, J.J. & Lee, G.U. Low Piconewton Towing of CNS Axons against Diffusing and Surface-Bound Repellents Requires the Inhibition of Motor Protein-Associated Pathways. *Sci. Rep.* **4**, 7128; DOI:10.1038/srep07128 (2014).